Rare Metal Materials and Engineering
Volume 50, Issue 10, October 2021
Available online at www.rmme.ac.cn

Science Press

Cite this article as: Lin Tao, Jin Liuping, Li Wenyuan, et al. Effect of Surface Coating on Porous Mg Scaffolds for Bone Engineering[J]. Rare Metal Materials and Engineering, 2021, 50(10): 3520-3526.

ARTICLE

Effect of Surface Coating on Porous Mg Scaffolds for Bone Engineering

Lin Tao[1], Jin Liuping[1], Li Wenyuan[1], Shao Huiping[1], Yuan Jiayun[1], Deng Xin[2,3]

[1] Institute for Advanced Materials & Technology, University of Science and Technology Beijing, Beijing 100083, China; [2] Guangdong University of Technology, Guangzhou 510006, China; [3] Jihua Laboratory, Foshan 528299, China

Abstract: Porous magnesium (Mg) scaffolds are beneficial to biological implantation, but because of the high activity of Mg, the degradation rate after implantation is too fast, which is not conducive to the formation of new bone. In order to effectively control the degradation of Mg scaffolds, three different surface coatings, magnesium oxide (MgO), calcium hydrogen phosphate (DCPD) and stearic acid (SA) on the porous Mg scaffolds was prepared and their effects on the scaffolds were investigated. The surface composition of the uncoated scaffold and the coatings was confirmed to be pure Mg, MgO, DCPD and SA by energy dispersive spectrometer (EDS), X-ray diffraction (XRD) and Fourier transforms infrared spectra (FTIR). The results show that SA coating is smoother and more compact in surface morphology. In vitro degradation in simulated body fluid (SBF) indicates that surface coatings can effectively slow down the scaffold degradation, while DCPD coating and SA coating are better than MgO coating in resisting the degradation. The degradation rate of the scaffolds with DCPD and SA coating soaked in SBF is 70% at the 15th week, which provides a certain period of time for the growth of new bone.

Key words: Mg scaffolds; coating; DCPD; SA; degradation behavior

More and more patients suffer from bone defects, nonunion and osteomyelitis due to trauma, tumors, bone diseases, etc. Bone tissue engineering provides an alternative new approach for the treatment of bone defects. Mg has great advantages in the application of bone tissue engineering materials because of its safety[1,2], bioactivity[3], degradability[4,5] and mechanical properties like human bone[6,7]. However, Mg is very active in chemical properties, its standard electrode potential is low (-2.37 V)[8], so it is easily corroded in body fluids containing chloride ions[9]. Therefore, surface treatment of porous Mg scaffolds is necessary to improve its corrosion resistance, so that the degradation rate of the scaffold matches the growth rate of the new bone. At present, the methods for Mg substrate surface treatment as a biological material mainly include micro-arc oxidation[10-13], alkali heat treatment[14-16], calcium orthophosphates coating[17-22], natural organic coating[23-26], etc.

In this study, uncoated porous Mg scaffolds prepared by 3D gel-printing (3DGP) [27-31] have the advantages of high solid loading, low cost, high efficiency, and wide range of materials, and are immersed in acid solution to remove surface impurities which are generated by degreasing and sintering. MgO coating on the surface of pure Mg scaffolds was prepared by oxidation in a high temperature furnace. Oxide coatings have a passivating effect on the corrosion of Mg, but the preparation of oxide coatings is mostly electrodeposition[32]. And DCPD coating and SA coating of Mg scaffolds were prepared by chemical deposition. The preparation of the DCPD coating is easier than other methods such as electrodeposition and the preparation process is easy to control. The resulting coating is uniform and has good adhesion[33]. The stearic acid coating has no micro-cracks, and its surface is very smooth, which can provide effective protection for magnesium from corrosion[34]. Compared with the modification of the magnesium coating previously studied, the preparation of the coating in this experiment is simple and the cost is low. The purpose of this study is to find a more suitable coating against their degradation behavior in SBF in vitro.

Received date: October 26, 2020
Foundation item: Jihua Laboratory Project (X190061UZ190); Science and Technology Projects of Guangdong Province (2016B090914001)
Corresponding author: Lin Tao, Ph. D., Associate Professor, Institute for Advanced Material & Technology, University of Science and Technology Beijing, Beijing 100083, P. R. China, E-mail: lintao@ustb.edu.cn

1 Experiment

1.1 Experimental materials

According to our previous study[27], the porous uncoated Mg scaffolds prepared by 3DGP were used as substrate materials in this study. The viscosity curve of the slurry used in 3DGP is shown in Fig. 1a. It shows that the viscosity of the printing slurry decreases as the shear rate increases, and finally stabilizes, which allows the slurry to be smoothly extruded at the needle. The reversibility of shear thinning of the plastic fluid enables the printing wire to maintain its original shape without deformation after being squeezed out of the needle, thereby achieving layer-by-layer printing. The printing parameters are set as follows: the needle size is 0.7 mm, the layer height is 0.6 mm, the printing wire moving speed is 10 mm/s, and the printing wire pitch is 0.65 mm. Fig. 1b shows the substrate material and experimental uncoated Mg scaffolds. The width of the printing wire is 2 mm, and the pore diameter is about 2 mm. The experimental scaffolds were smaller scaffolds with a size of 6 mm×8 mm× 8 mm, which were cut from the substrate.

Absolute ethanol, concentrated nitric acid, concentrated hydrochloric acid, calcium nitrate, ammonium dihydrogen phosphate, chemical oleic acid, stearic acid, chromium trioxide, silver nitrate, were all AR and came from Sinopharm Chemical Reagent Co., Ltd. Mg powder (Tangshan Weihao Magnesium Powder Co., Ltd) and simulated body fluid (SBF, Beijing Leagene Biotechnology Co., Ltd) were used in this study. The impurity content of Mg powder used in this study is shown in Table 1.

The compressive strength and the elastic modulus were measured by a universal testing machine (Instron 3366).

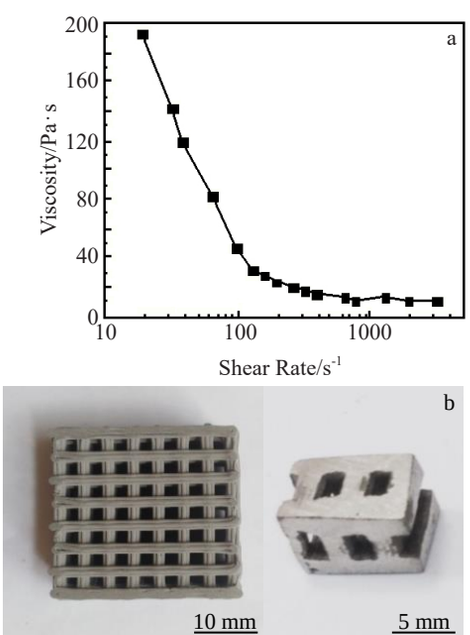

Fig.1 Viscosity curve of the printing slurry (a) and images of uncoated Mg scaffolds (b)

Table 1 Content of impurities in Mg powder (wt%)

Fe	Mn	Zn	Cl	Mg
0.045	0.008	0.008	0.004	Bal.

1.2 Surface modification process

Firstly, the experimental scaffolds were polished to 0.5 μm with SiC paper and diamond polishing agent to make the surface smooth for subsequent surface modification. Uncoated Mg scaffolds and three different kinds of surface coatings on porous Mg scaffolds were prepared as follows.

(1) Uncoated Mg scaffolds

The scaffolds were immersed in 5% nitric acid-5% hydrochloric acid alcohol solution for 1 min, and then placed in absolute ethanol to be ultrasonically cleaned. Acid immersion was used to remove oxides and impurities on the surface of the scaffolds. The uncoated porous Mg scaffolds were obtained after being dried.

(2) MgO coating

To prepare the surface oxidation coating, the dried uncoated Mg scaffolds were surface-oxidized in a tube furnace under the protection of pure argon mixed with trace oxygen according to the temperature curve shown in Fig.2.

(3) DCPD coating

The deposition solution was a deionized aqueous solution of 0.01 mol/L $Ca(NO_3)_2$ and 0.01 mol/L $NH_4H_2PO_4$ and the scaffolds were immersed in the solution for 3 d. The deposition solution needs to be placed in a water bath to maintain a constant temperature of 37 ℃ and replaced every 12 h.

(4) SA coating

The deposition procedure in order to prepare SA coatings required two-steps. The first step is that Mg scaffolds were placed in the oleic acid under vacuum condition to improve the wettability of Mg matrix, and then maintained at room temperature for 15 min. The second step is that the scaffolds were immersed in SA at 100 ℃ for 30 min after being dried. The sample types are shown in Table 2.

1.3 In vitro biodegradation behavior in SBF

In order to study the degradability and biosafety of the coated scaffolds, in vitro SBF immersion experiments were

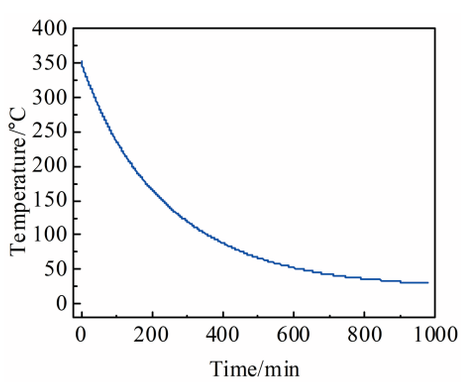

Fig.2 Relation curve between temperature and oxidation time

Table 2 Four different kinds of samples

Sample	Description
1	Uncoated porous Mg scaffolds
2	Porous Mg scaffolds with MgO coating
3	Porous Mg scaffolds with DCPD coating
4	Porous Mg scaffolds with SA coating

performed. Five samples of the same coated scaffolds were selected for in vitro SBF degradation testing. Behavior of four different kinds of samples (uncoated, MgO coating, DCPD coating and SA coating) was compared.

The scaffolds were immersed in 20 mL simulated body fluid at 37 ℃, and then the mass loss was measured in degradation experiment in vitro. Before being weighed, the scaffolds were cleaned with ASTM G1 standard chromic acid solution (200 g/L CrO_3 and 10 g/L $AgNO_3$) and thoroughly dried to remove surface degradation products and residual liquid.

Remaining mass percentage (P_i, %) is used to describe the degradation of the samples. It can be estimated by the following formula:

$$P_i = \frac{W_i}{W_o} \times 100\%$$

where W_O is the mass of the original sample (g), W_i is the mass of the sample at the i day (g), i is the number of experimental days when the sample is taken out to be measured.

1.4 Characterization

The surface morphologies of the samples were observed by scanning electron microscopy (SEM, ZEISS EVO®18, Carl Zeiss NTS, Germany) and confocal laser scanning microscope (CLSM, OLYMPUS LEXTOLS4000). The composition and structure of the coatings were tested by energy dispersive spectrometer (EDS, LEO1450), X-ray diffraction (XRD, DMAX-RB) and Fourier transforms infrared (FTIR) spectra (Nicolet IS50).

2 Results and Discussion

2.1 Properties of Mg scaffold substrate

Table 3 shows the density, compressive strength and the elastic modulus of uncoated Mg substrate scaffolds and cancellous bone. As shown in Table 3, the density of Mg scaffolds is slightly lower than that of cancellous bone, the compressive strength meets the standard of cancellous bone, and the elastic modulus of Mg scaffolds is close to that of cancellous bone. The porosity of Mg scaffolds is very close to that of cancellous bone and its pore diameter is larger than that of cancellous bone, which is beneficial to the growth of the bone tissue.

Table 3 Properties of uncoated Mg scaffolds and cancellous bone

Property	Mg scaffold	Cancellous bone[35-37]
Density/g·cm^{-3}	0.72±0.07	1.8~2.1
Compressive strength/MPa	8.05±1.28	0.1~16
Elastic modulus/MPa	0.32±0.02	0.5~20
Pore diameter/mm	2.0±0.1	0.4~0.6
Porosity/%	58.6±4.1	40.0~60.0

2.2 Morphology and phase identification

Fig. 3 shows SEM images and EDS analysis of four different samples. Fig. $3a_1$ shows the surface morphology of porous uncoated Mg scaffolds, and it is obvious that the entire surface is relatively smooth and sintered from a single original powder. Fig. $3b_1$ shows the surface morphology of surface oxidation coating. A non-densified oxide layer is formed on the scaffolds surface. Fig. $3c_1$ shows the surface morphology of DCPD coating. The deposited coating on the scaffolds surface is an irregular sheet-like and plate-like dense interwoven structure that is tightly bonded to the substrate. Fig. $3a_2$ and Fig. $3b_2$ show that the oxygen content on the coating surface is significantly increased. It can be seen from Fig. $3c_2$ that elements such as Ca, P, and O are deposited on Mg scaffolds surface. Fig. $3d_2$ shows that besides Mg, more O and C elements appear on the surface. Fig. $3d_1$ shows SEM image of SA coatings; due to the low secondary electron yield of organic matter under tungsten scanning electron microscopy, the coating morphology cannot be seen clearly. Therefore, the laser confocal microscope was used, and the image is shown in the upper right corner of Fig. $3d_1$. SA coating surface is like bamboo leaves, which is smoother and more compact, and has almost no gap with the substrate. The surface of the scaffold is not very smooth, which is conducive to SA to adhere to the surface of the scaffold and fill the grooves on the surface of the scaffold[38]. SA is hydrophobic and can slow down the corrosion of the stent in the SBF[39]. At the same time, SA is non-toxic and has good biocompatibility[26].

In order to analyze the Mg scaffold surface coatings, XRD and FTIR analyses were carried out. Fig. 4 shows XRD analysis of four different samples. The diffraction peaks of the uncoated scaffolds at diffraction angles of 32°, 34°, and 36° are typical peaks of Mg (PDF No. 65-0476). Peaks of the surface oxidation coating have a typical peak of magnesium oxide at 43° and 62° (PDF No. 65-0476) in addition to Mg typical peak. Peaks of DCPD coating at diffraction angle of 12°, 34°, 72° are typical peaks of DCPD (PDF No. 72-1240). As shown in the curve of SA coating, there is no typical peak of SA, but typical Mg peaks at diffraction angles of 34° and 36° are found. To further confirm the composition of the coating, the samples were subjected to FTIR spectrum.

Fig. 5 shows FTIR spectra curves of the samples. Combined with EDS and XRD, it can be found that there is no other phase on the surface of the uncoated sample. As shown in the spectrum of surface oxidation coating, the peaks at 501 cm^{-1} can be attributed to MgO. From the spectra of EDS, XRD and FTIR of sample 2, it can be concluded that surface coating is magnesium oxide. The spectrum of the DCPD coating is in accordance with the standard FTIR spectrum of $CaHPO_4 \cdot 2H_2O$. The absorbance bands of 3545 and 3480 cm^{-1} are for crystal water of $CaHPO_4 \cdot 2H_2O$[40]. The peak at 1646 cm^{-1} is for H-O-H. The presence of bands at 1135 and

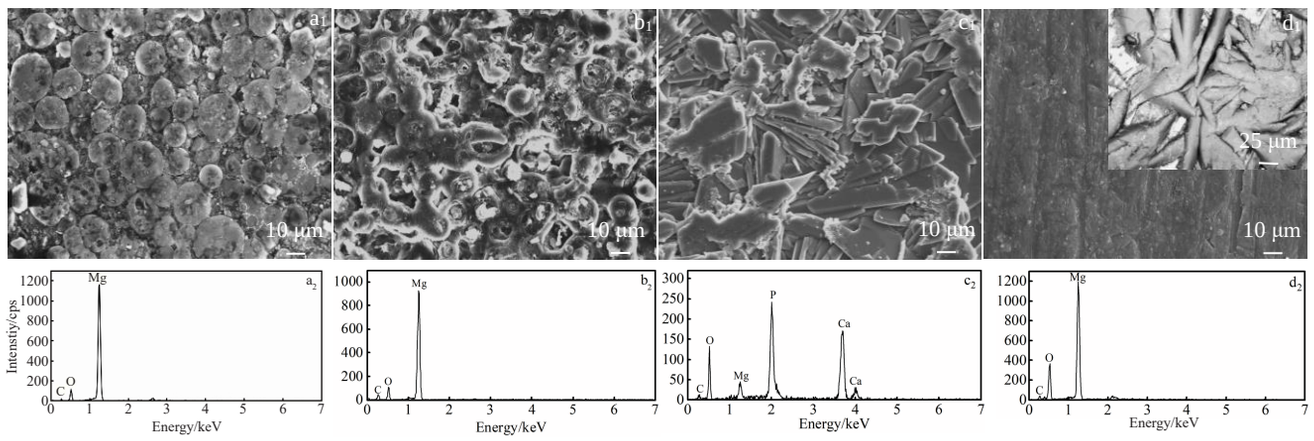

Fig.3 SEM images and EDS spectra of the samples: (a_1, a_2) uncoated scaffold, (b_1, b_2) surface oxidation coating, (c_1, c_2) DCPD coating, and (d_1, d_2) SA coating

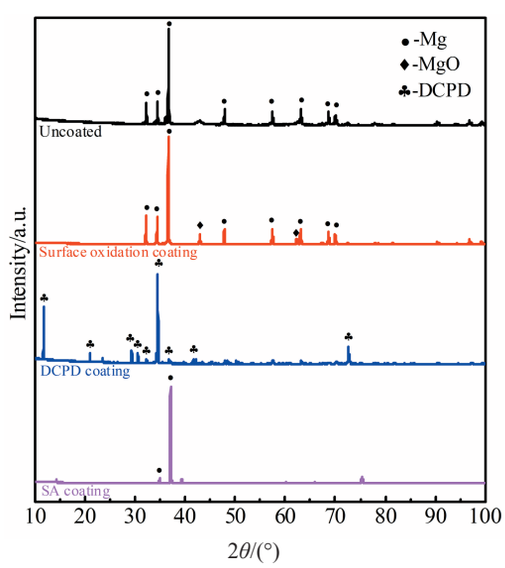

Fig.4 XRD patterns of different coating samples

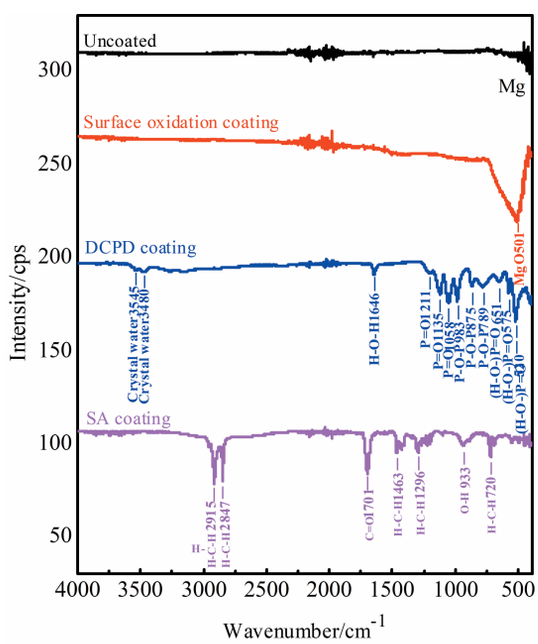

Fig.5 FTIR spectra of the samples

1211 cm^{-1} is related to the P=O stretching modes and the band at 1058 cm^{-1} is due to the P=O bending vibrations. The peaks of 983, 875 and 789 cm^{-1} can be attributed to P-O-P asymmetrical stretching modes[40]. The peaks of 651, 575 and 520 cm^{-1} are related to (H-O-) P=O[40]. From the spectra of EDS, XRD and FTIR of sample 3, it can be concluded that DCPD coating is deposited on the substrate. The spectrum of SA coating is in accordance with the standard FTIR spectrum of stearic acid. The peaks of 2915 and 2847 cm^{-1} are for CH_3 and CH_2 group of SA, respectively. The peak of 1701 cm^{-1} is for C=O group of SA[41]. Also, the peaks of 1463, 1296 and 720 cm^{-1} are typical peaks of CH_2 of SA. Therefore, it can be indicated that SA is deposited on the porous Mg scaffolds.

Fig. 6 shows cross-sectional morphologies of uncoated and three different coatings on porous Mg scaffolds. As shown in Fig. 6a, there is some powder at the boundary of the cross section of the scaffold. And as shown in Fig.6b and Fig.6d, the junction of MgO coating and SA coating is relatively smooth, and these two coatings cannot be observed under SEM. Fig.6c shows that the thickness of DCPD coating is 16~28 μm, and there are a few cracks in the coating, without obvious large cracks.

2.3 In vitro biodegradation performances in SBF

Fig. 7 shows the in vitro degradation curve of four different samples in SBF. The degradation speed of uncoated sample is too fast and other three coatings greatly improve the degradation properties. In the first week after implantation of the scaffolds, the reduction in the mass of the three scaffolds with different coatings is similar to a loss rate of about 10%, but in the second week to eighth week, the degradation of the three scaffolds with different coatings is gradually different. The mass of the oxidized scaffolds is rapidly decreased and only 20% of the original mass is remained at the 8th week.

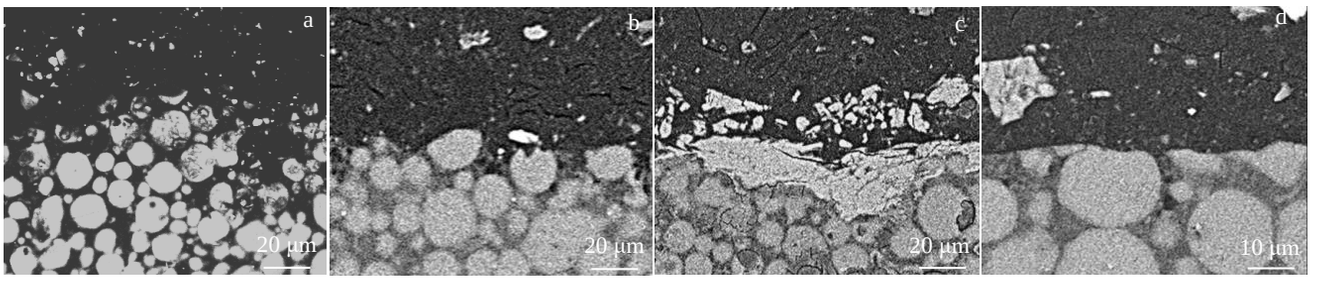

Fig.6 Cross-sectional morphologies of the scaffolds with different coatings: (a) uncoated, (b) MgO, (c) DCPD, and (d) SA

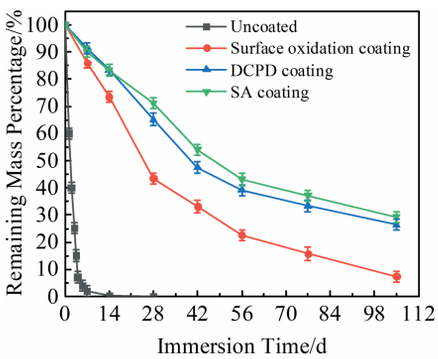

Fig.7 In vitro degradation curves of the samples in SBF

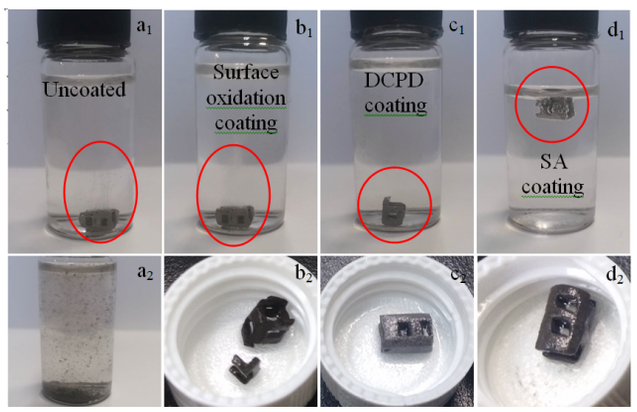

Fig.8 Scaffold uncoated immersed in the SBF at initial state (a_1) and for 1 min (a_2); scaffolds with different coatings immersed in SBF solution at initial state (b_1~d_1) and for 2 weeks (b_2~d_2): (a_1, a_2) uncoated scaffold, (b_1, b_2) surface oxidation coating, (c_1, c_2) DCPD coating, and (d_1, d_2) SA coating

The mass loss of the scaffolds with DCPD coating and SA coating is significantly slower which is 40% at the 8th week. After 8 weeks, the degradation of the three kinds of scaffolds with different coatings becomes stable. The degradation of the scaffolds is consistent with the surface morphology analysis of the coating shown in Fig. 3. It can be seen from Fig. $3b_1$ that there are large oxidation pits between the formed surface oxide coatings and the structure is relatively loose, which cannot completely isolate the scaffold from reacting with SBF. However, compared with Fig.$3a_1$, the area in contact with SBF is greatly reduced, so the degradation rate slows down. It can be seen from Fig. $3c_1$ and Fig. $3d_1$ that the coating layer is needle-shaped, which is denser than the surface oxidation coating and can effectively reduce the degradation rate.

Fig. $8a_1$~$8d_1$ show that the scaffolds with different coatings immersed in SBF solution in vitro at initial state. The ratio of the scaffold mass to the SBF volume is 0.1∶6. Table 4 shows the mass of four different kinds of scaffolds and the SBF volume. As shown in the red mark of Fig. $8a_1$, black powder appears on the surface of the scaffold, which is caused by degradation in the SBF. As shown in the red mark of Fig. $8b_1$, the surface of the scaffold produces many small bubbles in the SBF, which indicate that the oxide coating is loose. As shown in the red mark of Fig. $8c_1$, the surface of the scaffold has no reaction, indicating that the DCPD coating deposition is uniform and dense. As shown in the red mark of Fig. $8d_1$, the scaffold floats on the liquid surface, which is due to the lower density of SA (0.847g/cm^3), and the surface of the scaffold has also no reaction, indicating that the SA coating deposition is also uniform and dense.

Table 4 Mass of four different scaffolds and SBF volume

Sample	Scaffold mass/g	SBF volume/mL
Uncoated	0.142	8.5
Surface oxidation coating	0.155	9.3
DCPD coating	0.161	9.6
SA coating	0.132	7.9

Fig. $8a_2$ shows the uncoated scaffold immersed in the SBF for 1 min and Fig. $8b_2$~$8d_2$ show three different coated scaffolds immersed in SBF solution for 2 weeks. As shown in Fig. $8a_2$, the scaffold is completely degraded to powder and loses its mechanical strength. As shown in Fig. $8b_2$, small part of the scaffold with the surface oxidation coating is broken in the SBF but the overall scaffold still has certain strength, which indicates that the corrosion is uneven due to the unevenness of the oxidation coating surface. As shown in Fig. $8c_2$ and $8d_2$, the outline of the scaffolds with DCPD coating and SA coating becomes smoother at the edges, which means that the edges and corners are more likely to corrode, and the corrosion is relatively slow in the smooth areas.

In vitro biodegradation property in SBF of Mg scaffolds is

improved significantly via depositing DCPD coating and SA coating. In vitro biodegradation property in SBF of Mg scaffolds with SA coating is slightly better than with DCPD coating.

3 Conclusions

1) For the Mg scaffold, its surface oxidation coating is loose, DCPD coating is an irregular sheet-like and plate-like dense interwoven structure and SA coating is a smooth and compact bamboo leaf structure.

2) Compared with the uncoated Mg scaffolds, other three types of coatings can effectively slow down the degradation rate of Mg scaffolds, and DCPD and SA coatings are better than the surface oxidation coating.

3) In the first week after implantation of the scaffolds, the reduction in the mass of the three scaffolds with different coatings is similar, with a loss rate of about 10%, but in the second week to eighth week, the in vitro degradation in SBF of the three scaffolds with different coatings is gradually different. The degradation of the scaffolds with SA coating is slightly better than that of the scaffolds with DCPD coating, and the remaining mass is about 40% of the initial value at the 8th week. After 8 weeks, the degradation of the three types of coatings becomes stable. It is obvious that the surface coatings of Mg scaffolds can effectively slow down the in vitro degradation rate in SBF and provide a certain period of time for the growth of new bone.

References

1 Lsaris Nils-Erik, Mervaala Eero, Karppanen Heikki *et al. Clinica Chimica Acta*[J], 2000, 294(1): 1

2 Hartwig Andrea. *Mutation Research/Fundamental and Molecular Mechanisms of Mutagenesis*[J], 2001, 475(1): 113

3 Federica I Wolf, Achille Cittadini. *Molecular Aspects of Medicine*[J], 2003, 24(1): 3

4 Udhayan R, Bhatt Devendra Prakash. *Journal of Power Sources* [J], 1996, 63(1): 103

5 Witte F, Kaese V, Haferkamp H *et al*. *Biomaterials*[J], 2005, 26(17): 3557

6 Zhang Runfang, Liu Debao, Li Hua *et al. Rare Metal Materials and Engineering*[J], 2018, 47(9): 2833

7 Gibson L J. *Journal of Biomechanics*[J], 1985, 18(5): 317

8 Tang Zibo, Niu Jialin, Huang Hua *et al. Journal of the Mechanical Behavior of Biomedical Materials*[J], 20197, 72: 182

9 Gao Jiacheng, Li Longchuan, Wang Yong *et al. Rare Metal Materials and Engineering*[J], 2005, 30(4): 903

10 Aydin Hakan, Bayram Ali, Uguz Agah *et al. Materials Testing* [J], 2008, 50(6): 318

11 Liu G Y, Hu J, Ding Z K *et al. Applied Surface Science*[J], 2011, 257(6): 2051

12 Liu Guangyi, Tang Shanwei, Li Dechao *et al. Corrosion Science* [J], 2014, 79: 206

13 Ramin Rojaee, Mohammadhossein Fathi, Keyvan Raeissi. *Applied Surface Science*[J], 2013, 285(15): 664

14 Gu X N, Zheng W, Cheng Y *et al. Acta Biomaterialia*[J], 2009, 5(7): 2790

15 Al-Abdullat Y, Tsutsumi S, Nakajima N *et al. Materials Transactions*[J], 2001, 42(8): 1777

16 Li Longchuan, Gao Jiacheng, Wang Yong *et al. Surface and Coatings Technology*[J], 2004, 185(1): 92

17 Ong Joo L, Chan Daniel. *Critical Reviews in Biomedical Engineering*[J], 2000, 28(5): 667

18 Anselme K. *Biomaterials*[J], 2000, 21(7): 667

19 Liu Yuelian, Klaas de Groot, Ernst B Hunziker. *Frontiers of Materials Science in China*[J], 2009, 3: 154

20 Zhang Yajing, Zhang Guozhi, Mei Wei *et al. Journal of Biomedical Materials Research Part B Applied Biomaterials*[J], 2010, 89B(2): 408

21 Wang Yong, Mei Wei, Gao Jiacheng. *Materials Science and Engineering C*[J], 2009, 29(4): 1311

22 Waterman J, Pietak A, Birbilis N *et al. Materials Science and Engineering B*[J], 2011, 176(20): 1756

23 Gu X N, Zheng Y F, Lan Q X *et al. Biomedical Materials*[J], 2009, 4: 1

24 Ye C H, Zheng Y F, Wang S Q *et al*. *Applied Surface Science*[J], 2012, 258(8): 3420

25 Ng W F, Wong M H, Cheng F T. *Surface and Coatings Technology*[J], 2010, 204(11): 1823

26 Hornberger H, Virtanen S, Boccaccini A R. *Acta Biomaterialia* [J], 2012, 8(7): 2442

27 Ren Xiangyuan, Shao Huiping, Lin Tao *et al*. *Materials & Design*[J], 2016, 101: 80

28 Shao Huiping, Zhao Dechao, Lin Tao *et al*. *Ceramics International* [J], 2017, 43(16): 13 938

29 Shao Huiping, He Jiangzhuang, Lin Tao *et al. Ceramics International*[J], 2019, 45(1): 1163

30 Zhang Yumeng, Shao Huiping, Lin Tao *et al. Ceramics International*[J], 2019, 45(16): 20 493

31 Zhang Zhinan, Lin Tao, Shao Huiping *et al*. *Ceramics International*[J], 2020, 46(5): 6491

32 Zhen Xu, Ubong Eduok, Jerzy Szpunar. *Surface and Coatings Technology*[J], 2019, 357: 691

33 Tan Lili, Wang Qiang, Geng Fang *et al*. *Transactions of Nonferrous Metals Society of China*[J], 2010, 20(2): 648

34 Gupta R K, Mensah-Darkwa K, Sankar J *et al*. *Transactions of Nonferrous Metals Society of China*[J], 2013. 23(5): 1237

35 Hernandez C J, Beaupre G S, Keller T S *et al*. *Bone*[J], 2001, 29 (1): 74

36 Hara Daisuke, Nakashima Yasuharu, Sato Taishi *et al*. *Materials Science and Engineering C*[J], 2016, 59: 1047

37 Gao Huanyu, Li Yanlin, Xiao Yu *et al*. *Chinese Journal of Tissue Engineering Research*[J], 2016, 20: 6237

38 Chen Ningning, Wang Yanhua, Zhong Lian *et al*. *Chinese Journal of Materials Research*[J], 2017, 31(10): 751

39 Wang Yanhua, Wang Wei, Zhong Lian *et al*. *Applied Surface Science*[J], 2010, 256(12): 3837
40 Xu Liping, Zhang Erlin, Yang Ke. *Transactions of Nonferrous Metals Society of China*[J], 2012, 22(8): 2014
41 Zhang Xiaoxu, Li Qing, Li Longqin *et al*. *Materials Letters*[J], 2012, 88: 76

表面涂层对用于骨组织工程的多孔镁支架的影响

林　涛[1]，靳浏平[1]，李文媛[1]，邵慧萍[1]，袁佳昀[1]，邓　欣[2,3]
(1. 北京科技大学 新材料技术研究院，北京 100083)
(2. 广东工业大学，广东 广州 510006)
(3. 季华实验室，广东 佛山 528299)

摘　要：多孔镁（Mg）支架有利于生物植入，但是由于Mg的高活性，植入后降解速度过快，不利于新骨的形成。为了有效地控制镁支架的降解，研究了3种不同表面涂层对多孔镁支架的影响。通过能量色散光谱仪（EDS），X射线衍射（XRD）和红外傅里叶变换光谱（FTIR）证实支架表面的组成为纯Mg，氧化镁（MgO），磷酸氢钙（DCPD）和硬脂酸（SA）。结果表明，从表面形貌可以看出，SA涂层更光滑，更致密。模拟体液（SBF）的体外降解实验表明，与未涂覆的Mg支架相比，表面涂层可以有效地减慢支架的降解，并且DCPD涂层和SA涂层优于MgO涂层。在第15周时，浸泡在SBF中的DCPD和SA涂层支架的降解率为70%，这可以为新骨的生长提供一定的时间。

关键词：Mg支架；涂层；DCPD；SA；降解行为

作者简介：林　涛，男，1970年生，博士，副教授，北京科技大学新材料技术研究院，北京 100083，E-mail：lintao@ustb.edu.cn